REPORT DOCUMENTATION PAGE

Form Approved
OMB NO. 0704-0188

1. AGENCY USE ONLY (Leave Blank)	2. REPORT DATE	3. REPORT TYPE AND DATES COVERED
	2001	~~Reprint~~

4. TITLE AND SUBTITLE
Biomedical Application of Target Tracking in clutter

5. FUNDING NUMBERS
DAAD19-01-1-0594

6. AUTHOR(S)
Scott T. Acton

7. PERFORMING ORGANIZATION NAME(S) AND ADDRESS(ES)
University of Virginia
1001 N. Emmett St.
Charlottesville, VA. 22903-4833

8. PERFORMING ORGANIZATION REPORT NUMBER

9. SPONSORING / MONITORING AGENCY NAME(S) AND ADDRESS(ES)
U. S. Army Research Office
P.O. Box 12211
Research Triangle Park, NC 27709-2211

10. SPONSORING / MONITORING AGENCY REPORT NUMBER
41628.6-CI

11. SUPPLEMENTARY NOTES
The views, opinions and/or findings contained in this report are those of the author(s) and should not be construed as an official Department of the Army position, policy or decision, unless so designated by other documentation.

12 a. DISTRIBUTION / AVAILABILITY STATEMENT
Approved for public release; distribution unlimited.

12 b. DISTRIBUTION CODE

13. ABSTRACT (Maximum 200 words)

SEE ATTACHED REPORT

14. SUBJECT TERMS	15. NUMBER OF PAGES
	16. PRICE CODE

17. SECURITY CLASSIFICATION OR REPORT	18. SECURITY CLASSIFICATION ON THIS PAGE	19. SECURITY CLASSIFICATION OF ABSTRACT	20. LIMITATION OF ABSTRACT
UNCLASSIFIED	**UNCLASSIFIED**	**UNCLASSIFIED**	**UL**

Biomedical Application of Target Tracking in Clutter

Adam P. Goobic, Michael E. Welser, Scott T. Acton, and Klaus Ley
Virginia Image and Video Analysis (VIVA)
Department of Electrical Engineering
University of Virginia
Charlottesville, VA 22904 USA

Abstract

The movement of leukocytes (white blood cells) and their interaction with the endothelium (vessel wall) provides valuable information about the mechanism of inflammation and inflammatory disease. In order to investigate leukocyte motion within living animals, advanced automated tracking algorithms are requisite. We introduce military target tracking algorithms for the purpose of tracking cell movement. In 33 experiments, we compare the tracking performance of five trackers. The trackers tested include the centroid tracker, the correlation tracker, an enhanced centroid tracker, an enhanced correlation tracker and an active contour (snake) tracker. Of the five methods, the snake tracker proved to be the most robust method in terms of the highest percentage of frames tracked and the lowest root mean-squared error. The paper provides an overview of the five trackers and gives experimental results.

1. Introduction

A rolling leukocyte is an activated white blood cell that travels along the endothelium wall to the site of injury. Tracking rolling leukocytes during inflammation is critical for analysis of the inflammatory process. Previous methods used to track cell movements *in vitro* (in flow chambers) with centroid and correlation tracking algorithms were moderately successful, but proved insufficient *in vivo* (in living animals). Although intravital tracking is more difficult, it provides valuable characterization of the cell-vessel interaction that is not possible within a flow chamber. This paper compares the performance of the basic centroid and correlation trackers, enhanced centroid and correlation trackers, and an active contour-based snake tracker. This comparison evaluates the algorithm robustness for tracking cells within living animals using video microscopy.

Active contour-based tracking shows significant potential for *in vivo* applications. Since we know the general shape and scale of the cells to be tracked, we can constrain active contours to capture such shapes. Our initial study concludes that the snake tracker algorithm results are superior to the basic and enhanced centroid and correlation trackers. These snake algorithms will be further integrated into a robust automatic *in vivo* cell tracking system. Such a system would eliminate the current time-consuming technique of manual tracking to observe rolling leukocytes. Furthermore, automated tracking will remove investigator bias from tracking data.

2. Methods

We evaluated five trackers that represent a broad spectrum of tracking methodologies. The conventional centroid and correlation trackers are included in the study. Enhanced versions of the centroid and correlation trackers are also analyzed. Finally, we scrutinize a tracker based on active contours. Here, we briefly review the approach taken by each tracking system.

2.1 The Centroid Tracker

The first tracking algorithm implemented is a simple centroid tracker. The fundamental idea of the centroid tracker is to compute the "center of mass" within a subimage to locate the center of the target. Here, "mass" is the sum of intensities in the subimage called the *track gate*. We automatically compute the track gate boundary to bound the target cell. Within this track gate, we use the pixel intensities to calculate the center of mass. If sufficient contrast exists between the cell and the background, the centroid tracker gives reliable results. Where contrast varies or the scene is cluttered, the centroid is apt to lose track of the target cell. In the cluttered environment of intravital cell tracking, the centroid tracker is prone to locking on to brighter cells or to the endothelium (vessel wall).

This material is based upon work supported in part by the U. S. Army Research Laboratory and the U. S. Army Research Office under contract/grant number DAAD19-01-1-0594

2.2 The Correlation Tracker

The second tracking algorithm implemented is a basic correlation tracker. The fundamental idea of a correlation tracker is to locate the cell though template matching. Specifically, the correlation tracker creates a template of the leukocyte to be tracked from the initial track gate, then uses this template to find the highest normalized cross correlation measure within future frames to locate the cell position. For template T and subimage S, the normalized cross correlation at translation (a, b) is given by

$$c(a,b) = \frac{\sum_x \sum_y S(x-a, y-b)T(x,y)}{\sqrt{\left[\sum_x \sum_y S^2(x-a, y-b)\right]\left[\sum_x \sum_y T^2(x,y)\right]}} \quad (1)$$

The correlation tracker is straightforward to implement, and is able to detect objects that do not change size, shape, shade or move great distances from the previous frame. Because leukocytes *in vitro* remain relatively stable visually, the correlation is fairly successful in a flow chamber environment. However, the cluttered videos obtained *in vivo* are beyond the capability of this basic tracker.

2.3 The SuperCentroid Tracker

The third tracking algorithm tested is an enhanced centroid tracker called the *SuperCentroid.* The fundamental difference between SuperCentroid and the conventional centroid tracker is that SuperCentroid uses adaptive template matching to determine when the target object is lost. Adaptive template matching uses an adaptive target template to locate the object of interest by matching the template to the object in the image and allowing the most recent target image to gradually alter the template. Adaptive template matching gives the ability to track cells that change size, shape, and intensity due to cell deformation or camera focus, angle, and lighting. The template $\mathbf{T}_{k+1}$ is updated by taking a weighted average of the current track gate $\mathbf{O}_k$ with the current template $\mathbf{T}_k$:

$$\mathbf{T}_{k+1} = \gamma \mathbf{T}_k + (1-\gamma)\mathbf{O}_k \quad (2)$$

where both $\mathbf{T}_k$ and $\mathbf{O}_k$ are centered at the centroid.

2.4 The SuperCorrelation Tracker

The fourth tracking algorithm in the study is an enhanced correlation tracker called the *SuperCorrelation* tracker. SuperCorrelation, like the SuperCentroid, uses adaptive template matching. SuperCorrelation also uses the centroid to re-position the center of the template. In addition to the mechanism of adaptive template matching, both the SuperCentroid and the SuperCorrelation trackers utilize several additional enhancements.

2.5 Common Features of Enhanced Trackers

Both SuperCentroid and SuperCorrelation increase tracker robustness by implementing background removal, image enhancement and the Kalman filter. Background removal extracts non-moving features such as muscle, tissue, and other vessel walls. It is accomplished by time-averaging the video frames in a sequence and subtracting the averaged frame from each video frame while tracking.

Given that the cells are roughly circular in shape and have a known diameter, we can utilize morphological filters to further reduce clutter. We have used both morphological anisotropic diffusion [1] and standard morphological filters for enhancement. In this study, we report results with the standard morphological open-close filter:

$$\mathbf{E} = (\mathbf{I} \circ \mathbf{B}) \bullet \mathbf{B} \quad (3)$$

where $\mathbf{E}$ is the enhanced image, $\mathbf{I}$ is the input image, and $\mathbf{B}$ is a structuring element that is circular and set to be of smaller scale than the cells.

The third enhancement common to both the SuperCentroid and SuperCorrelation trackers is the use of a predictive filter for coasting. The *Kalman filter* provides a means to predict leukocyte movement when the leukocyte is obscured by clutter. Essentially, the Kalman filter uses the history of the leukocyte position to the position in the subsequent frame. If the tracker loses the target (as detected by poor correlation), the Kalman filter prediction can be used as the observation. In this case, we say that the tracker is *coasting*.

We form two Kalman filters for prediction: one for the horizontal position of the leukocyte and one for the vertical position of the leukocyte [2]. Let i_k be the row position of a cell at video frame k. Then

$$i_{k+1} = i_k + \delta t \; v_k^i \quad (4)$$

where δt is the time between frames (here 1/30 s) and v_k^i is the velocity. The predicted row position is

$$\hat{i}_{k+1|k} = \hat{i}_{k|k} + \delta t \; \hat{v}_{k+1|k}^i \quad (5)$$

where $\hat{i}_{k|k}$ is the filtered row position estimate, and $\hat{v}_{k+1|k}^i$ is the predicted velocity. Once we have tracked a cell for a few frames, the Kalman gains will give more weight to the predicted position and velocity over the observed position and velocity. The Kalman filter provides the minimum mean-squared error solution to the track position estimation and prediction

problem [2], given the assumption of a constant velocity target.

2.6 The Snake Tracker

The fifth tracking algorithm we implemented is an active contour or *snake* tracker. The snake algorithm tries to minimize an energy function based on internal snake energy (tension and rigidity), external energy (co-location with maxima in image gradient), shape, size, position, and sampling constraints. These constraints are weighted and combined into an energy functional [3]:

$$E_{\text{snake}} = \lambda_1 E_{\text{int}} + \lambda_2 E_{\text{ext}} + \lambda_3 E_{\text{shape}} + \lambda_4 E_{\text{size}} + \lambda_5 E_{\text{pos}} + \lambda_6 E_{\text{sampling}} \cdot \quad (6)$$

The internal energy is the bending/stretching energy that is minimized by low magnitudes of the first and second derivatives of the curve $\mathbf{C}(s)$ with respect to the parameter s. The external energy is minimized when the contour is located over the edge of a cell – the position of high gradient magnitude.

These snakes are well-suited for contrast-changing and shape-changing cells. Because we know shape size and position information about cells a *priori* we can incorporate these as parameters in our energy function to provide a more robust algorithm. Snake shape can be constrained to known elliptical and circular cell shapes. Snake size is known, because we know the approximate cell size from the scale of the video. Figure 1 shows the importance of the combination of the shape and size constraints in capturing a leukocyte for tracking.

The position constraint incorporates future cell positions as predicted by a Kalman filter. The snake used here is parametric, described by several (~100) discrete positions known as *snaxels*, which outline the target object. As the snake evolves with cell variations, the snaxel positions adjust to keep an even spacing around the target object boundary. In addition, the snake re-parameterizes itself (keeping uniform sampling) according to the sampling energy term. Euler equations derived from (6) provide updates for the (x, y) position of each snaxel [3].

The assumed initial radius of the snake tracker is integral to effective tracking. This parameter allows the snake to formulate the size constraint, which governs the relative size of the circle or ellipse shape constraint. An accurate value of the initial radius as compared to the actual radius of the target cell realizes a more effective snake tracker.

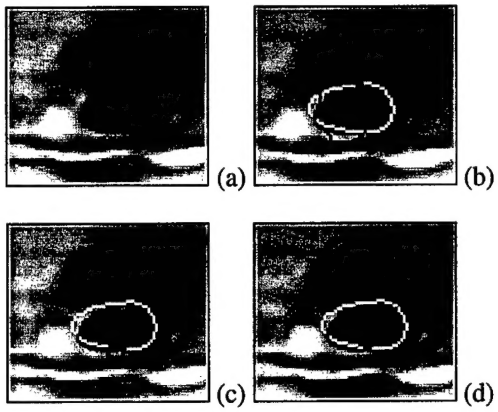

Figure 1: (a) Leukocytes within a video frame. (b) Tracking with shape constraint only. (c) Tracking with size constraint only. (d) Tracking with both shape and size constraints. The initial and the final snakes are shown in white and black respectively [3].

2.7 Tracker Performance Measures

We determine a tracker's performance by the percentage of frames tracked and the root mean-squared error (RMSE). The percentage of frames tracked is the number of frames tracked by the tracker divided by the number of frames the cell is in the video sequence. Here, we count a frame as "tracked" if the computed position is within one cell radius of the manually determined position. The RMSE (in microns) describes how accurately the tracker tracks the cell as compared to the "ground truth" data.

The combination of the percentage of frames tracked and the RMSE yields the qualitative performance ratings shown in Table 1.

Table 1: Tracker performance ratings

Performance Rating	% Frames Tracked	RMSE (microns)
Excellent	90-100	below 1
Good	75-89	1-2
Fair	60-74	3-5
Poor	below 60	above 5

3. Results and Conclusions

Our dataset consists of intravital microscopy video recordings of rolling leukocytes in the mouse cremaster muscle observed via transillumination. We tracked thirty-three cells from ten venules (small vessels). Five sets are TNF-α treated venules; five sets are untreated. The TNF-α treatment increases the inflammatory response and thus slows down the rolling cells. Such cells are then more easily tracked at the lower

velocities. Each video sequence contains the tracked cells for about 2 seconds (or for 60 frames at 30 frames/second). The efficacy of each tracker is determined by comparing experimental results with "ground truth" data – a manual frame-by-frame record of cell position. Currently all five trackers acquire the initial position from the first "ground truth" position value. We intend to integrate automatic cell identification in future tracking systems.

The snake tracker produced results with the smallest average RMSE and largest average percentage of frames tracked. The results attest to the snake tracker's robust ability to track cells in cluttered conditions. The snake tracker is able to overcome obstacles that inhibit the other trackers such as bright cells in the neighborhood of the target cell, low contrast with the background, and fast moving cells.

The numerical results yielded by the snake tracker prove the potential for a robust *in vivo* cell tracker. As shown in Figure 2, the snake tracker is able to track 100% of the frames in all 16 TNF-α data sets. In addition, the average RMSE for the 16 TNF-α sequences is 0.33 microns, for cells that measure ~10 microns in diameter. The performance of the SuperCorrelation tracker was acceptable, but the average RMSE of 1.94 is over five times that of the snake tracker. The SuperCentroid, centroid, and correlation trackers do not perform nearly as well as evidenced by Figure 2. In the untreated venules, the performance of the snake tracker drops to 48% of the frames tracked successfully. Nevertheless, the performance of the other four trackers also declines, with the SuperCentroid providing the next highest tracking percentage at 35%. In this case, the snake tracker also has the lowest RMSE by a margin of 7 microns.

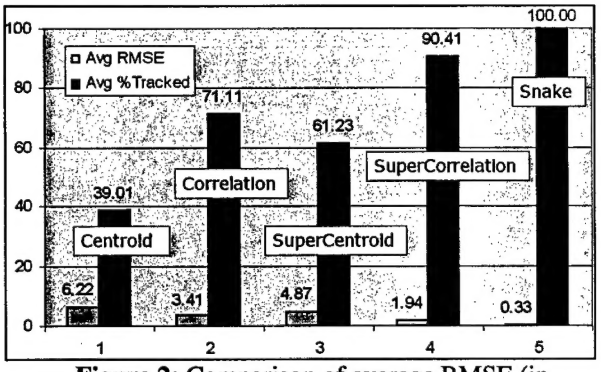

Figure 2: Comparison of average RMSE (in microns) and percent tracked for the experiments using treated venules.

Figure 3 displays the hand-tracked displacements of the target cell from the initial position (ground-truth), and each tracker's attempt to follow the cell for a TNF-α sequence. Clearly, the snake tracks the target cell more accurately than the other algorithms in this case. Similar results are observed from the other 32 data sets.

The snake tracker can be improved in the following areas: computational complexity, initial radius specification, and clutter-reducing methods. Currently, the snake tracker cannot produce results in real-time. For example, execution of the snake tracker on a ninety-frame sequence using a desktop machine with a Pentium 3 processor and 256MB of RAM takes 16 minutes to complete. Thus, the snake tracker needs about 13 hours to process 50 ninety-frame sequences. Eventually, we hope to design and implement a system that can process sequences at or near real time. To reduce computation time and attain this goal, we are investigating both hardware and algorithmic enhancements. The specific algorithmic enhancements include fast matrix inversion for calculation of the snake update equations.

Furthermore, the snake tracker will be made more robust once we can effectively and efficiently identify the initial radius of the cell. Presently, we use a range of radius values to achieve tracking for a given cell. More research is needed to develop a means to automatically provide the snake tracker with an initial cell radius. The snake tracker can be further improved by incorporating additional filters that remove clutter while maintaining target edges at a range of scales.

A user-friendly software package for laboratory application is another step in realizing a complete *in vivo* cell tracking system. We have prototyped the *Python*, a graphical user interface that allows user-friendly cell selection and automated tracking. The Python provides for manual target acquisition and specification of various tracking algorithms and clutter-reducing filters. A sample screen view of the Python is shown in Figure 4.

Snake-based algorithms show significant promise for future *in vivo* cell tracking. The ability to track rolling leukocytes *in vivo* will bolster research and development in anti-inflammatory drugs for diseases such as Crohn's disease and atherosclerosis.

References

[1] S.T. Acton and K. Ley, "Tracking leukocytes from *in vivo* video microscopy using morphological anisotropic diffusion," *Proc. IEEE Int. Conf. on Image Processing*, Thessaloniki, Greece, October 7-10, 2001.

[2] C.A. Segall, W. Chen, and S.T. Acton, "Video tracking using the morphological pyramid," *Journal of Electronic Imaging*, vol. 8, pp. 176-184, 1999.

[3] N. Ray, S.T. Acton, and K. Ley, "Tracking leukocytes *in vivo* with shape and size constrained active contours," submitted to *IEEE Transactions on Medical Imaging*, 2001

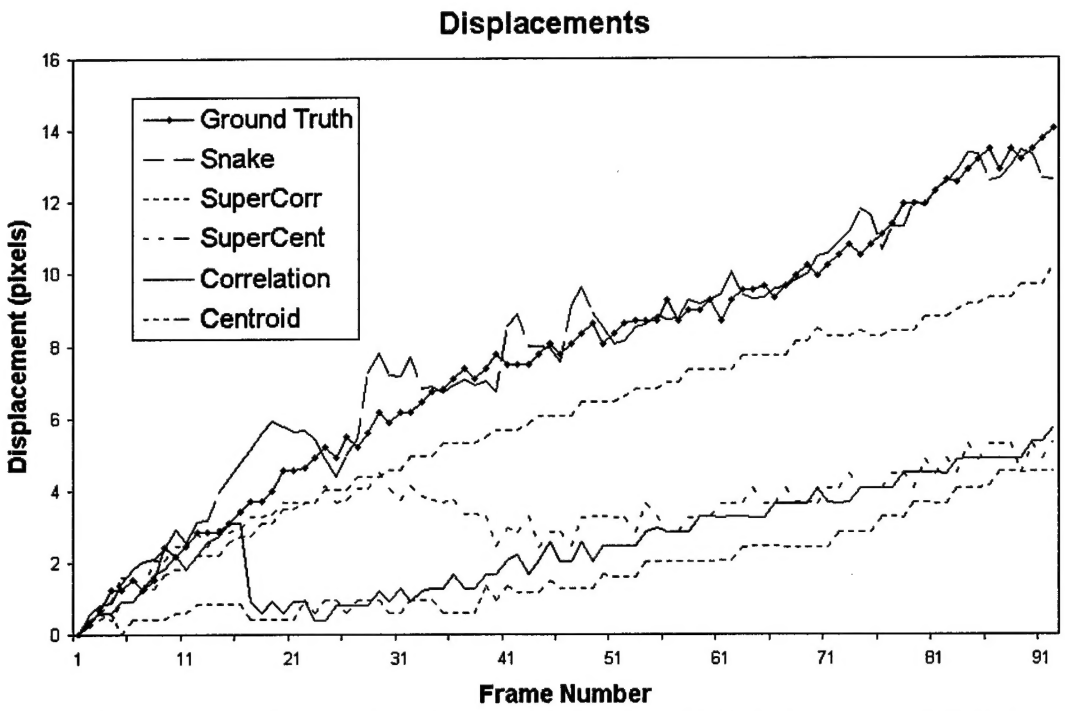

Figure 3: Comparison of tracker displacements for a sequence obtained from a TNF- α treated vessel.

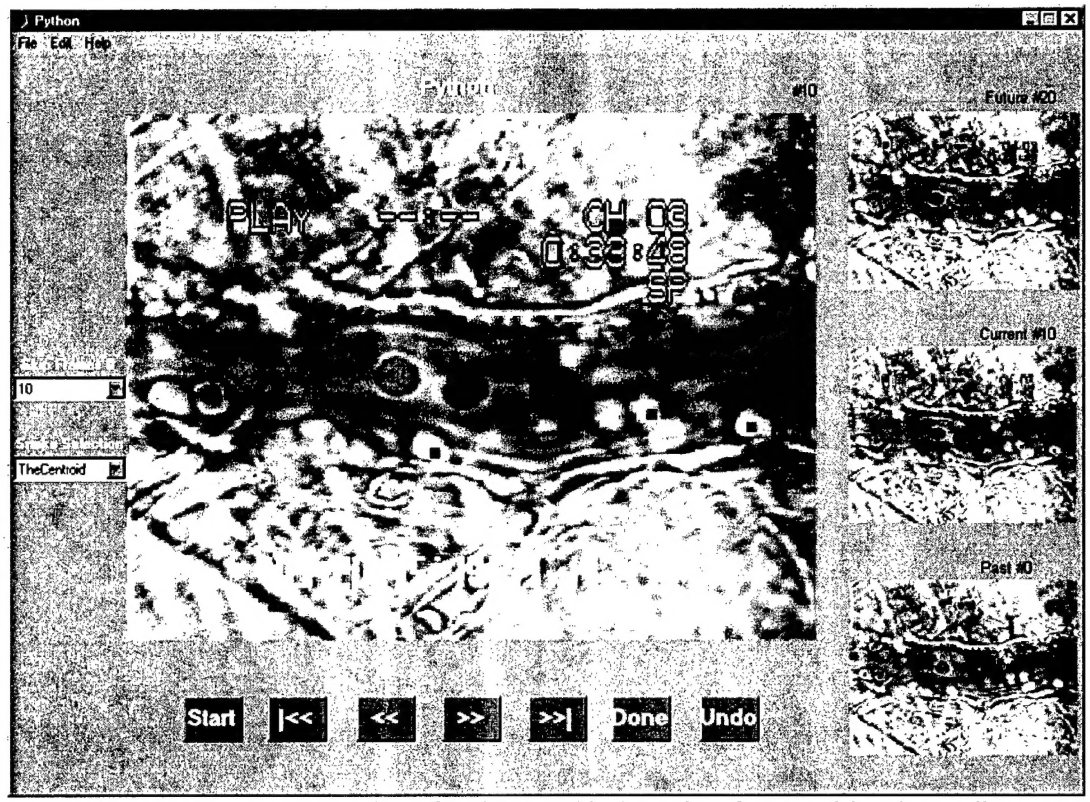

Figure 4: Sample screen view of Python graphical user interface acquiring three cells.

Acknowledgements

The authors thank N. Ray for his implementation of the snake tracker.